Spreading and epigenetic inheritance of heterochromatin require a critical density of histone H3 lysine 9 tri-methylation

Amber R. Cutter DiPiazza[a], Nitika Taneja[a,1], Jothy Dhakshnamoorthy[a], David Wheeler[a], Sahana Holla[a], and Shiv I. S. Grewal[a,2]

[a]Laboratory of Biochemistry and Molecular Biology, National Cancer Institute, NIH, Bethesda, MD 20892

Edited by Steven E. Jacobsen, University of California, Los Angeles, CA, and approved April 20, 2021 (received for review January 12, 2021)

Heterochromatin assembly requires methylation of histone H3 lysine 9 (H3K9me) and serves as a paradigm for understanding the importance of histone modifications in epigenetic genome control. Heterochromatin is nucleated at specific genomic sites and spreads across extended chromosomal domains to promote gene silencing. Moreover, heterochromatic structures can be epigenetically inherited in a self-templating manner, which is critical for stable gene repression. The spreading and inheritance of heterochromatin are believed to be dependent on preexisting H3K9 tri-methylation (H3K9me3), which is recognized by the histone methyltransferase Clr4/Suv39h via its chromodomain, to promote further deposition of H3K9me. However, the process involving the coupling of the "read" and "write" capabilities of histone methyltransferases is poorly understood. From an unbiased genetic screen, we characterize a dominant-negative mutation in histone H3 ($H3^{G13D}$) that impairs the propagation of endogenous and ectopic heterochromatin domains in the fission yeast genome. $H3^{G13D}$ blocks methylation of H3K9 by the Clr4/Suv39h methyltransferase and acts in a dosage-dependent manner to interfere with the spreading and maintenance of heterochromatin. Our analyses show that the incorporation of unmethylatable histone $H3^{G13D}$ into chromatin decreases H3K9me3 density and thereby compromises the read-write capability of Clr4/Suv39h. Consistently, enhancing the affinity of Clr4/Suv39h for methylated H3K9 is sufficient to overcome the defects in heterochromatin assembly caused by $H3^{G13D}$. Our work directly implicates methylated histones in the transmission of epigenetic memory and shows that a critical density threshold of H3K9me3 is required to promote epigenetic inheritance of heterochromatin through the read-write mechanism.

heterochromatin | epigenetic | histone methylation | gene silencing

The assembly of distinct chromatin domains within eukaryotic genomes facilitates diverse chromosomal processes, including the maintenance of genome stability, and the regulation of gene expression, DNA replication and recombination. Histones and their posttranslational modifications are components of epigenetic mechanisms that partition the genome into "open" euchromatin or "closed" heterochromatin domains (1–3). Euchromatin domains, marked by histone acetylation and histone H3 lysine 4 methylation (H3K4me), are generally more accessible to transcription machinery, whereas repressive heterochromatin domains are hypoacetylated and contain the histone H3 lysine 9 methylation (H3K9me) mark (4, 5). Histone H3 proteins bearing di- and tri-methylation marks (H3K9me2/3) are recognized by heterochromatin protein 1 (HP1) family proteins (6–8), which together serve as a recruitment scaffold for multiple effectors (2). Considering that histone modifications define gene expression patterns specific to different cell types, determining their role in the assembly and propagation of distinct chromatin domains is critical for understanding normal development and disease states.

The fission yeast *Schizosaccharomyces pombe* is an excellent model system for studying heterochromatin assembly. Small facultative heterochromatin islands target developmentally and environmentally regulated genes, and large constitutive heterochromatin domains coat pericentromeric, subtelomeric, and the silent mating-type (*mat*) regions (9–12). Heterochromatin assembly is a multistep process that includes nucleation and spreading. The de novo nucleation of heterochromatin occurs at specific sites, such as repeat elements within constitutive heterochromatin domains, from where heterochromatin factors spread to surrounding sequences (13, 14). RNAi machinery (13, 15), as well as factors involved in nuclear RNA processing and noncanonical RNA polymerase II termination (12, 16–19), nucleate heterochromatin by targeting the multisubunit Clr4 methyltransferase complex (ClrC) (20) that is responsible for mono-, di-, and tri-methylation of histone H3K9 (H3K9me1/2/3) (6, 21). Clr4 has a unique dual activity allowing it to bind to methylated H3K9 via its chromodomain ("read") and catalyze H3K9 methylation ("write"), a feature that is essential for heterochromatin to spread (22, 23). The H3K9me2/3 marks also provide a binding site for other chromodomain proteins, including the HP1 family members Chp2 and Swi6 (24), which in turn target effectors such as the Snf2-histone deacetylase (HDAC) repressor complex (SHREC) involved in transcriptional gene silencing (25, 26).

The principle that preexisting heterochromatin can be epigenetically inherited in a self-templating manner during both mitosis and meiosis was uncovered through studying heterochromatin

Significance

In multicellular organisms, a single genome gives rise to a multitude of cell types by enforcing appropriate gene expression patterns. Epigenetic mechanisms involving modification of histones, including tri-methylation of histone H3 lysine 9 (H3K9me3), assemble and propagate repressive heterochromatin to prevent untimely gene expression. Dysregulation of epigenetic gene-silencing mechanisms is a hallmark of a variety of diseases including cancer. However, the requirements for epigenetic transmission of heterochromatin are not well understood. This study reveals the mechanism by which methylated histones provide an epigenetic template for heterochromatin propagation. We discover that a critical threshold of H3K9me3 is required for effective chromatin-association of the histone methyltransferase, which binds to and catalyzes additional H3K9me to propagate heterochromatin and enforce stable gene silencing.

Author contributions: A.R.C.D. and S.I.S.G. designed research; A.R.C.D., N.T., and J.D. performed research; A.R.C.D. and J.D. contributed new reagents; A.R.C.D., N.T., D.W., S.H., and S.I.S.G. analyzed data; and A.R.C.D. and S.I.S.G. wrote the paper.

The authors declare no competing interest.

This article is a PNAS Direct Submission.

[1]Present address: Department of Molecular Genetics, Erasmus MC Cancer Institute, Erasmus University Medical Center, 3000 CA Rotterdam, The Netherlands.

[2]To whom correspondence may be addressed. Email: grewals@mail.nih.gov.

This article contains supporting information online at https://www.pnas.org/lookup/suppl/doi:10.1073/pnas.2100699118/-/DCSupplemental.

Published May 25, 2021.

assembly at the silent *mat* region in *S. pombe* (13, 27, 28). Further insights into epigenetic transmission of chromatin structure soon followed. The first major finding established the importance of Clr4 read-write activity in the epigenetic inheritance of heterochromatin (22). This work showed that parental H3K9 methylated nucleosomes and their associated factors are a "molecular bookmark" and provide an epigenetic template for loading Clr4 (via the Clr4 chromodomain) to promote clonal propagation of heterochromatin. Another key finding was that constitutive heterochromatin domains show markedly lower turnover of histones compared to euchromatin domains and that the suppression of histone turnover preserves epigenetic memory for the inheritance of heterochromatin (29). The HDAC Clr3 and the homolog of mammalian SMARCAD1, Fft3, are recruited by HP1 proteins or other factors and stabilize nucleosomes carrying H3K9me, thus promoting stable propagation of heterochromtin (29, 30). Moreover, the nuclear peripheral subdomain provides an ideal microenvironment for loading factors that facilitate epigenetic inheritance (31, 32). Despite significant progress, evidence directly linking methylated histones to epigenetic memory and a detailed molecular mechanism underlying heterochromatin inheritance have yet to emerge.

Here, we report that a mutant isolated from our previous genetic screen affects heterochromatin propagation (30). The mutation maps to one of three genes encoding histone H3 and converts glycine residue 13 to aspartic acid in the H3 amino-terminal tail ($H3^{G13D}$). $H3^{G13D}$, which cannot be methylated by Clr4, acts in a dominant-negative manner to impair the spreading and epigenetic inheritance of heterochromatin. $H3^{G13D}$ is distinct from the previously described $H3^{K9M}$ dominant mutation that enhances the association between the catalytic SET (SUVAR3-9, Enhancer-of-zeste and Trithorax) domain of the methyltransferase and the H3 tail, thereby trapping Clr4 and blocking H3K9me (33). Rather, our work shows that $H3^{G13D}$ reduces the density of the H3K9me3 mark, which is recognized by Clr4 to further promote deposition of H3K9me. We find that enhancing the affinity of Clr4 for H3K9me2 nucleosomes is sufficient to overcome the heterochromatin defects caused by $H3^{G13D}$. These results demonstrate that epigenetic propagation of heterochromatin relies on a critical density threshold of H3K9me3 to promote Clr4 read-write activity. Our findings may also elucidate how mutations in histone tails, including those linked to cancer (34–39), perturb the chromatin landscape in cells.

Results

***EMS32* Harbors a Mutation in *hht2* that Affects Heterochromatin Maintenance.** The heterochromatin domain comprising the silent mating-type loci *mat2P* and *mat3M* and the interval between them (referred to as the *K*-region) serves as a paradigm for understanding the assembly and maintenance of repressive chromatin. Heterochromatin nucleated at the centromere-homologous *cenH* element spreads across the ~20 kb region surrounded by *IR-L* and *IR-R* inverted repeat elements (5, 13) (Fig. 1*A*). Cells in which the nucleation center *cenH* is replaced with *ura4*$^+$ (*KΔ::ura4*$^+$) establish heterochromatin stochastically. Once assembled, the heterochromatic state is stably propagated in cis via a mechanism involving suppression of histone turnover and Clr4 read-write activity (13, 22, 27–30, 32). The *KΔ::ura4*$^+$ reporter allows the identification of factors whose requirement in heterochromatin propagation is otherwise masked by de novo nucleation mechanisms.

We characterized the *EMS32* mutant identified in our previous genetic screen using the *KΔ::ura4*$^+$ reporter (Fig. 1*A*) (30). *EMS32* conferred a strong silencing defect in the *KΔ::ura4*$^+$ background, but only weakly affected the expression of the *Kint2::ura4*$^+$ reporter in which de novo assembly mechanisms are functional (Fig. 1*B*). The silencing defects correlated with severe reduction in both H3K9me2 and H3K9me3 levels at the *mat* locus in *EMS32 KΔ::ura4*$^+$ cells (Fig. 1*C*). By contrast, *EMS32 Kint2::ura4*$^+$ cells showed a modest reduction in H3K9me3 with a concomitant increase in H3K9me2. The reduction in H3K9me3 and H3K9me2 occurred throughout the silent *mat* region in *EMS32 KΔ::ura4*$^+$ cells (Fig. 1*D*). Additionally, *EMS32* exhibited reduced H3K9me at facultative heterochromatin islands (*SI Appendix*, Fig. S1) as well as changes in H3K9me levels at subtelomeric and pericentromeric regions (Fig. 1*D*). These analyses indicate that *EMS32* compromises heterochromatin assembly in cells defective in de novo heterochromatin nucleation at the silent *mat* region, specifically by affecting the propagation of heterochromatin domains.

To map the *EMS32* mutation, we backcrossed *EMS32* to a non-mutagenized parental strain and performed tetrad analyses in which silencing of the *ura4*$^+$ reporter was monitored to isolate wild-type (WT) and *EMS32* segregants. Whole-genome sequencing and nucleotide variant analysis of three WT and three *EMS32* segregants revealed a G-to-A nucleotide substitution unique to *EMS32* mutants that mapped to *hht2*. In *S. pombe,* the histone H3 protein is encoded by three alleles, *hht1*$^+$, *hht2*$^+$, and *hht3*$^+$ (40). Conventional DNA sequencing confirmed the G-to-A nucleotide conversion in *hht2* (Fig. 2*A*), which changes glycine to aspartic acid at position 13 (G13D) in the amino-terminal tail of histone H3.

$H3^{G13D}$ Has a Dominant-Negative Effect on Heterochromatin. To further investigate $H3^{G13D}$, we used a highly sensitive reporter to detect heterochromatin changes at the silent *mat* region. Deletion of a local silencer *REII*, which acts redundantly with heterochromatin to silence *mat2P*, facitilates detection of heterochromatin assembly defects (32, 41, 42). In nonswitching *mat1-M* cells lacking the *REII* element, impaired heterochromatic silencing of *mat2P* leads to "haploid meiosis," an aberrant sporulation phenotype resulting from coexpression of *M* and *P* mating-type information in haploid cells. Haploid meiosis is detected by exposing yeast colonies to iodine vapor. Colonies undergoing haploid-meiosis stain dark brown when exposed to iodine vapor, whereas WT colonies appear yellow. The *ura4*$^+$ reporter inserted near *mat2P* (*mat2P::ura4*$^+$) provides an additional readout for heterochromatic silencing. Consistent with defects in heterochromatin maintenance, *REIIΔ hht2*^{G13D} cells showed de-repression of *mat2P* and the *ura4*$^+$ reporter (Fig. 2*B*). $H3^{G13D}$ did not impact the expression of histone H3 or its incorporation into chromatin (*SI Appendix*, Fig. S2 *A–C*). Importantly, deletion of *hht2* in the mutant strain restored silencing and heterochromatin-specific H3K9me2/3, indicating that *hht2*^{G13D} is a dominant-negative mutation (Fig. 2*B* and *SI Appendix*, Fig. S2*D*). Notably, unlike the uniform de-repression of *mat2P* and the *ura4*$^+$ reporter in cells lacking Clr4, *hht2*^{G13D} exhibited a variegated phenotype, with single colonies showing a mixture of light and dark staining, and a smaller proportion of cells undergoing haploid meiosis (Fig. 2*C*). Together, these results indicate that *hht2*^{G13D} is a dominant-negative mutation associated with heterochromatin and gene-silencing defects.

$H3^{G13D}$ Impairs Heterochromatin Spreading and Propagation. The variegated phenotype of *hht2*^{G13D} cells is reminiscent of other mutants with defects in heterochromatin propagation, including *fft3Δ* and *amo1Δ* (30, 32, 42). To test if similar defects could explain the phenotype of *REIIΔ hht2*^{G13D} cells, we mapped H3K9me2 and H3K9me3 at the silent *mat* region. Importantly, *hht2*^{G13D} cells showed a considerable reduction in H3K9me3, notably at regions distal to the *cenH* nucleation center (Fig. 2*D*). At *cenH*, H3K9me3 was only marginally reduced and correlated with an increase in H3K9me2 (Fig. 2*D*), consistent with the results described above (Fig. 1). ChIP-qPCR (Chromatin immunoprecipitation-quantitative polymerase chain reaction) analysis confirmed these results (Fig. 2*E*).

We then asked if *hht2*^{G13D} affects the localization of the ClrC methyltransferase complex, which spreads from *cenH* to surrounding sequences via the Clr4 read-write mechanism (22). Indeed, cells carrying *hht2*^{G13D} showed a considerable decrease in the epitope-tagged ClrC component Raf2 in the regions surrounding *cenH* (Fig. 2 *D* and *E*). This result is consistent with $H3^{G13D}$

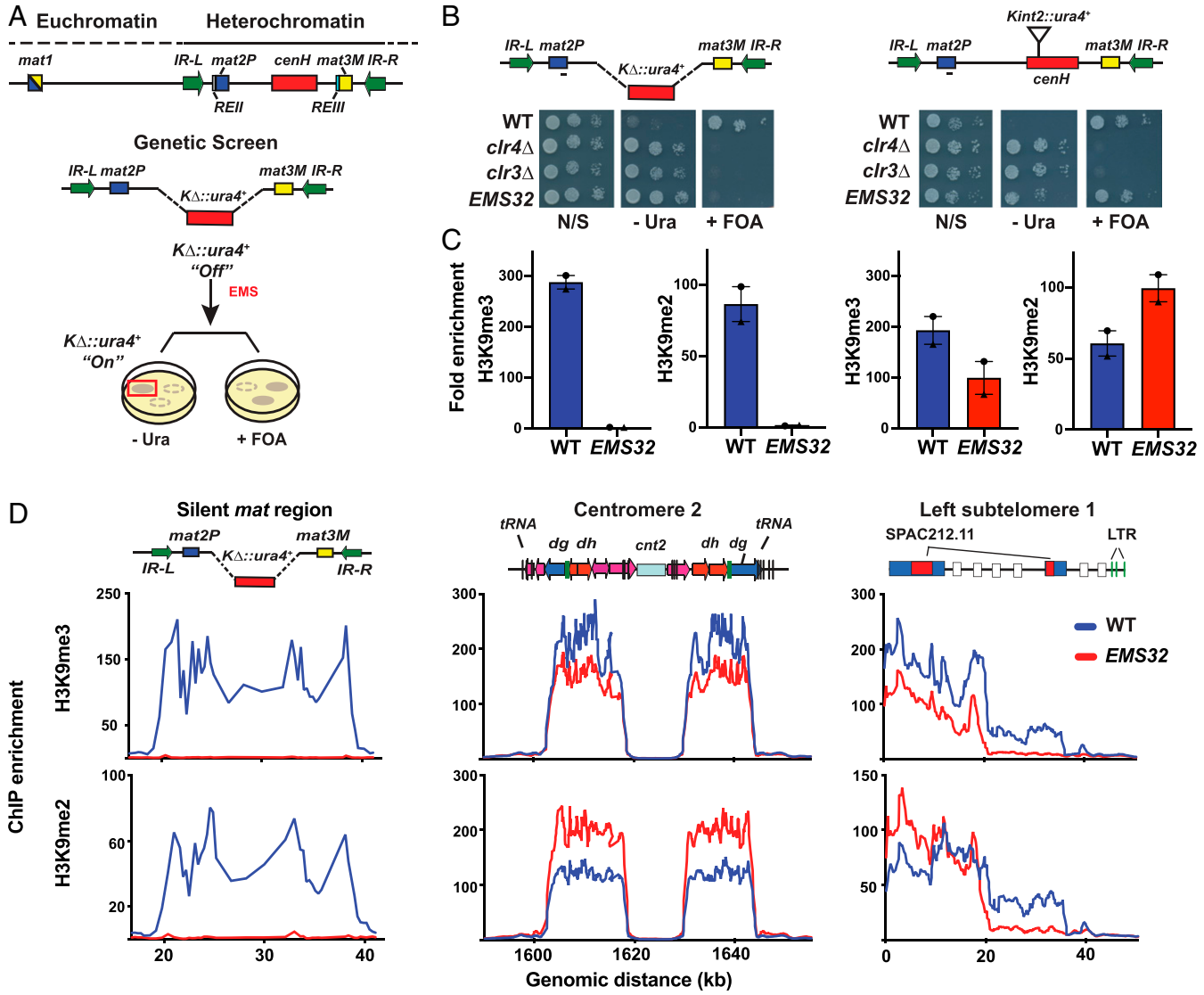

Fig. 1. Identification of a mutation that affects the maintenance of heterochromatin. (*A*) Schematic of the *S. pombe* mating-type (*mat*) locus (*Top*). Genetic screen using *KΔ::ura4*$^+$ cells to identify factors that affect the maintenance of heterochromatin (*Bottom*). (*B*) Expression analysis of *KΔ::ura4*$^+$ (*Left*) and *Kint2::ura4*$^+$ (*Right*) in the indicated strain backgrounds. (*C*) ChIP-qPCR (mean ± SEM; $n = 2$) of *KΔ::ura4*$^+$ (*Left*) and *Kint2::ura4*$^+$ (*Right*) strains. The fold enrichment of H3K9me3 and H3K9me2 at *mat2P* is shown for WT and the *EMS32* mutant background. (*D*) ChIP-chip analysis of H3K9me3 and H3K9me2 enrichment at heterochromatic loci in the indicated *KΔ::ura4*$^+$ strains. See also *SI Appendix*, Fig. S1.

interfering with the spreading and/or maintenance of heterochromatin by hindering Clr4 read-write activity.

We next tested whether *hht2*^{G13D} affects the propagation of heterochromatin at an ectopic site. We used an inducible system wherein cells express Clr4 fused to a TetR^{off} DNA-binding domain (TetR-Clr4) and harbor an *ade6*$^+$ reporter located downstream of six tetracycline operators (*6xtetO-ade6*$^+$). Following the release of TetR-Clr4 in cells lacking the anti-silencing factor Epe1 (43), heterochromatin at the ectopic site can be maintained for multiple generations via a mechanism involving the read-write activity of endogenous Clr4 (32, 44, 45). Cells expressing H3^{G13D} showed impairment of the epigenetic maintenance of heterochromatin at the ectopic site (Fig. 2*F*). This is consistent with identification of *hht2*^{G13D} as a mutant that affects heterochromatic silencing at an ectopic site (46). Importantly, *hht2*^{G13D} mutant cells showed a considerable reduction in H3K9me3 at the ectopic domain (Fig. 2*G*). Thus, H3^{G13D} impairs heterochromatin maintenance at both endogenous and ectopic sites.

Mutation of Shelterin Components Mitigates the Effect of H3^{G13D} on Heterochromatin. To better understand the mechanism by which H3^{G13D} affects heterochromatin formation, we employed an unbiased genetic screen that relies on the *REIIΔ mat2P::ura4*$^+$ reporter system to identify suppressors of the H3^{G13D} silencing defect. Mutagenesis was followed by screening for colonies that showed suppression of the haploid meiosis phenotype and the ability to grow on counter selective medium containing 5-fluoroorotic acid (FOA). Several suppressor candidates were isolated (*SI Appendix*, Fig. S3*A*), backcrossed, and subjected to tetrad analyses. Suppressor mutations were identified by whole-genome sequencing and nucleotide variant analysis. Interestingly, suppressor mutations mapped to genes encoding the Shelterin components Taz1, Ccq1, and Rap1 (*SI Appendix*, Fig. S3 *A* and *B*). Consistently, *taz1Δ*, *ccq1Δ*, or *rap1Δ* could also suppress the silencing defects in H3^{G13D} cells (Fig. 3*A*). The suppression was linked to partial restoration of heterochromatin as indicated by the increase in H3K9me2/3 levels at the silent *mat* region in *taz1Δ hht2*^{G13D} compared with *hht2*^{G13D} alone (Fig. 3*B*).

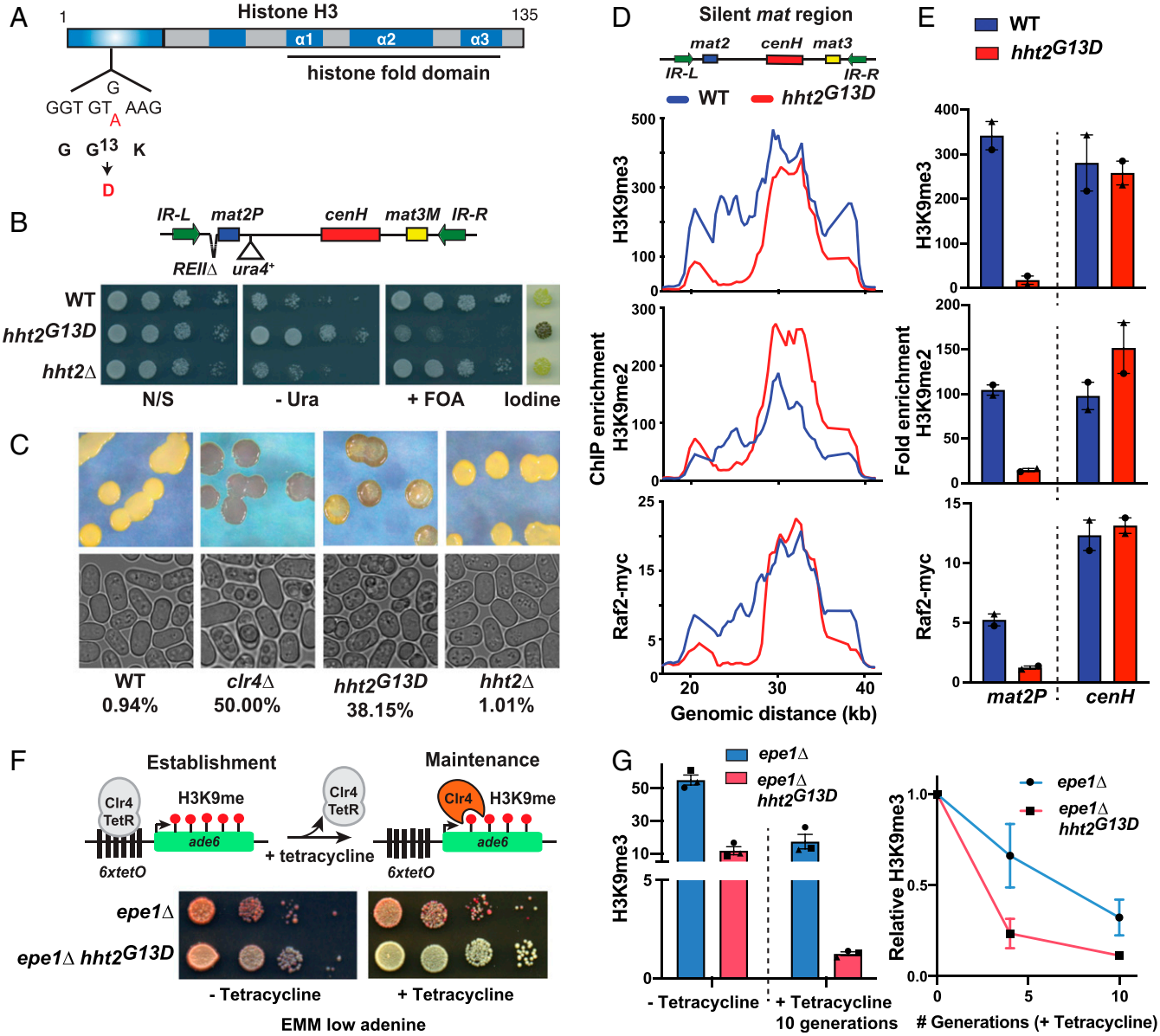

Fig. 2. *EMS32* is a dominant-negative mutation in histone H3 that disrupts the spreading and inheritance of heterochromatin. (*A*) Schematic of histone H3. Solid blue boxes indicate alpha-helices, and the gradient blue box represents the unstructured amino-terminal region. The position of the missense mutation associated with *EMS32* is indicated. (*B*) Expression analysis of *mat2P::ura4*$^{+}$ in the indicated strain backgrounds. *hht2*^{G13D} was deleted to construct *hht2Δ*. Additionally, PMG plates were stained with iodine vapor to detect haploid meiosis. (*C*) Representative images of single colonies subjected to iodine staining and live-cell microscopy are shown. The percentage of cells undergoing haploid meiosis (n = 225) is indicated. (*D*) ChIP-chip analysis of H3K9me3 (*Top*), H3K9me2 (*Middle*), and Raf2-myc (*Bottom*) enrichment at the silent *mat* region in the indicated *REIIΔ mat2P::ura4*$^{+}$ strains using a sliding window average of three probes. (*E*) ChIP-qPCR (mean ± SEM; n = 2) showing fold enrichment of H3K9me3, H3K9me2, and Raf2-myc at *mat2P* or *cenH* in the indicated *REIIΔ mat2P::ura4*$^{+}$ strains. (*F*) Schematic illustrating the establishment and maintenance of heterochromatin at an ectopic site with endogenous Clr4 indicated in orange (*Top*). Expression analysis in the indicated TetR-Clr4-expressing *6xtetO-ade6*$^{+}$ strain backgrounds (*Bottom*). (*G*) H3K9me3 ChIP-qPCR of strains grown in EMM+tetracycline media for 0, 4, and 10 generations (mean ± SEM; n = 3). Fold enrichments (*Left*) were calculated relative to *vps33*. Relative fold enrichments (*Right*) were calculated from fold enrichments compared to 0 generations. See also *SI Appendix*, Fig. S2.

Shelterin forms a complex with ClrC and is involved in heterochromatin assembly at telomeres and other loci (47–50). When Shelterin-mediated heterochromatin assembly is compromised, silencing factors are released and redistributed to other heterochromatic loci (51). Therefore, loss of Shelterin components might suppress heterochromatin defects in H3^{G13D} cells by increasing the available pool of silencing factors, such as Clr4, at the *mat* locus. Indeed, our attempts to identify *EMS32* by complementation using a genomic DNA library yielded several *clr4*$^{+}$-containing clones as suppressors of the silencing defect. Consistently, insertion of 3 to 4 copies of *clr4*$^{+}$ into the genome partially suppressed the silencing and heterochromatin defects in *hht2*^{G13D} (Fig. 3 *C* and *D*). Together, these results show that increasing the available pool of Clr4 is sufficient to partially overcome the inhibitory effect of H3^{G13D} on heterochromatin assembly at the silent *mat* region.

H3^{G13D} Impairs H3 Lysine 9 Methylation by Clr4. We next introduced the G13D mutation into a strain carrying a single copy of the histone H3 gene, *hht2*$^{+}$ (52). The single copy *hht2*^{G13D} cells exhibited de-repression of the *ade6*$^{+}$ reporter inserted at the

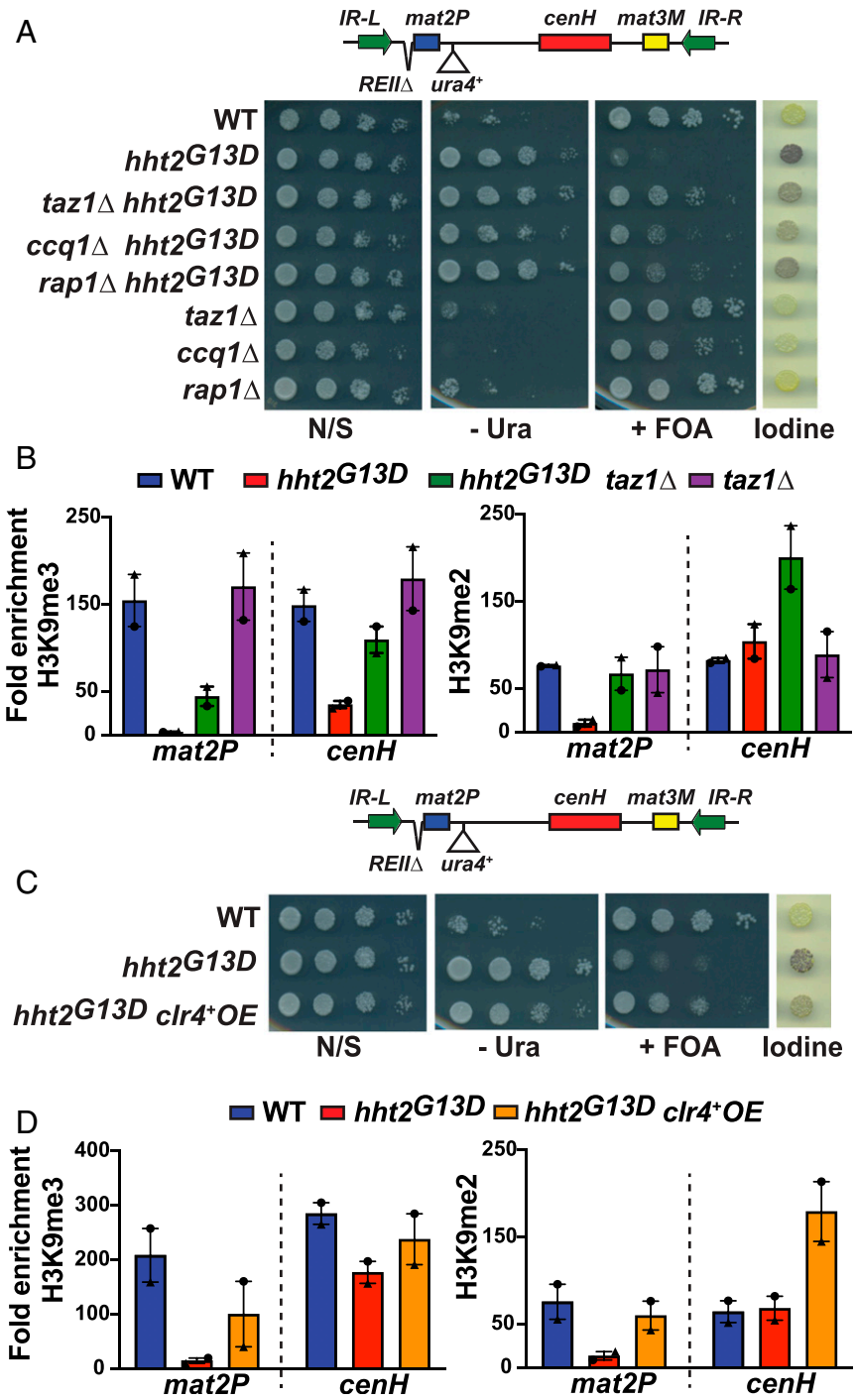

Fig. 3. Heterochromatin silencing defects in *hht2*^{G13D} mutant cells can be suppressed by increasing the local Clr4 concentration. (*A*) Expression analysis of *mat2P::ura4*$^{+}$ in the indicated strain backgrounds. Additionally, PMG plates were stained with iodine vapor to detect haploid meiosis. (*B*) ChIP-qPCR (mean ± SEM; $n = 2$) showing the fold enrichment of H3K9me3 and H3K9me2 at *mat2P* and *cenH* in the indicated *REIIΔ mat2P::ura4*$^{+}$ strains. (*C*) Expression analysis of *mat2P::ura4*$^{+}$ in the indicated strain backgrounds as described in *A*. OE indicates multiple copies of *clr4*$^{+}$ at the endogenous locus. (*D*) ChIP-qPCR analysis of the indicated strains (mean ± SEM; $n = 2$) as described in *B*. See also *SI Appendix*, Fig. S3.

outer pericentromeric repeat (*otr1R::ade6*$^{+}$), similar to cells in which H3K9 was mutated to arginine or alanine (Fig. 4*A*) (52). Unlike cells in which only one of the three copies of histone H3 was mutated (Fig. 1*D*), single-copy *hht2*^{G13D} cells showed a complete loss of H3K9me2/3 at pericentromeric repeats (Fig. 4*B*). Consistent with the loss of H3K9 methylation in vivo, Clr4 was unable to methylate the H3^{G13D} substrate in vitro (Fig. 4*C* and *SI Appendix*, Fig. S4). These results suggest that *hht2*^{G13D} affects heterochromatin assembly by preventing the methylation of H3K9 by Clr4, thereby reducing the requisite level of H3K9 methylated nucleosomes for Clr4 read-write activity.

Relative Abundance of H3^{G13D} Potentiates H3K9me Spreading and Gene-Silencing Defects. Since Clr4 binds to and catalyzes methylation of H3K9 to propagate heterochromatin (22, 23), the unmethylatable H3^{G13D} might "poison" the system by decreasing the

density of H3K9me3 critical for Clr4 read-write activity. To test this, we increased the relative abundance of $H3^{G13D}$ by placing epitope-tagged WT H3 or $H3^{G13D}$ under the control of the thiamine repressible *nmt1* promoter and monitored silencing at the *mat* region in *REIIΔ* background cells. H3 expression increased upon reduction of the thiamine concentration. Remarkably, an increase in $H3^{G13D}$, but not WT H3, corresponded with an increase in the haploid meiosis phenotype (Fig. 5 *A* and *B* and *SI Appendix*, Fig. S5*A*), indicating defective heterochromatic silencing. The silencing defect correlated with a decrease in H3K9me3 levels (Fig. 5 *C* and *D*). In particular, an increase in $H3^{G13D}$, but not WT protein levels, was linked to a concomitant reduction in the spreading of H3K9me3 to regions surrounding the *cenH* heterochromatin nucleation center at the silent *mat* region (Fig. 5*C* and *SI Appendix*, Fig. S5*B*). These results suggest that $H3^{G13D}$ acts in a dosage-dependent manner to interfere with heterochromatin spreading.

Enhanced Affinity of Clr4 for H3K9me Suppresses Heterochromatin-Spreading Defects. $H3^{G13D}$ likely affects heterochromatin spreading by compromising the read-write activity of Clr4 (22). However, $H3^{G13D}$ could trap Clr4 by stably binding to its catalytic SET domain, similar to $H3^{K9M}$ (33). To determine if interference with read-write activity is the primary defect, we attempted to suppress the heterochromatin defects in $H3^{G13D}$ cells by enhancing Clr4 binding to methylated H3K9. Clr4 sequentially catalyzes mono-, di- and trimethylation of H3K9; however, the conversion of H3K9me2 to H3K9me3 occurs relatively inefficiently and is the most sensitive to compromised Clr4 read-write activity (23). Consistently, $hht2^{G13D}$ cells showed a disproportionate reduction in H3K9me3 levels and a considerable enrichment of H3K9me2 (Figs. 1 and 2 *D* and *E*). To enhance Clr4 binding in $hht2^{G13D}$ cells, we replaced the Clr4 chromodomain (CD) with the Chp1 CD (Fig. 6*A*), which binds H3K9me2 with high affinity (23, 53). The expression of the $Clr4^{Chp1CD}$ chimeric protein under the control of native $clr4^{+}$ gene promoter had no effect on cell viability or *REIIΔ mat2P::ura4*$^{+}$ reporter gene silencing. Remarkably, $Clr4^{Chp1CD}$ suppressed the silencing defect at the *mat* locus in $hht2^{G13D}$ cells (Fig. 6*B*). This suppression corresponded with an increase in the levels of H3K9me3 and Raf2 across the silent *mat* interval (Fig. 6*C*) and subtelomeric heterochromatic domains (*SI Appendix*, Fig. S6*A*). These results indicate that $H3^{G13D}$ disrupts heterochromatin spreading by interfering with the read-write activity of Clr4 (Fig. 7). Interestingly, $Clr4^{Chp1CD}$ expression also led to a considerable increase in H3K9me2/3 at heterochromatin islands (*SI Appendix*, Fig. S6*B*), indicating that factors influencing the binding of Clr4 to methylated nucleosomes control the stability of facultative heterochromatin domains.

We then tested if $Clr4^{Chp1CD}$ could restore heterochromatic silencing in other mutants with reduced H3K9me3 levels, including cells lacking the FACT (Facilitates Chromatin Transcription) subunit Pob3, the SMARCAD1 homolog Fft3, or Amo1 involved in nuclear peripheral tethering of heterochromatin. Remarkably, $Clr4^{Chp1CD}$ suppressed the silencing defect in all three mutants (*SI Appendix*, Fig. S7*A*). We then expressed $Clr4^{Chp1CD}$ in $hht2^{K9M}$ mutant cells (33). The introduction of the $hht2^{K9M}$ mutation into *REIIΔ mat2P::ura4*$^{+}$ cells resulted in the loss of heterochromatic silencing at the silent *mat* region (*SI Appendix*, Fig. S7 *A* and *B*). Unlike cells expressing $H3^{G13D}$, the silencing defect in cells expressing $H3^{K9M}$ could not be rescued by $Clr4^{Chp1CD}$ (*SI Appendix*, Fig. S7 *A* and *B*). Thus, the mechanism by which $H3^{K9M}$ influences heterochromatin is likely distinct from that involving $H3^{G13D}$. Ultimately, the characterization of this unique mutant $hht2^{G13D}$ allele has revealed that a critical threshold of preexisting H3K9me3 is required for propagation of heterochromatin by the read-write activity of Clr4.

Discussion

The spreading of heterochromatin from nucleation sites to surrounding regions, and the epigenetic inheritance of these repressive structures, enforces genome stability and stable gene repression during development. We previously described how suppression of histone turnover by activities such as HDACs stabilizes H3K9me nucleosomes (29, 30), which provide an epigenetic template for anchoring Clr4 via its chromodomain to clonally propagate heterochromatin (22). Additional factors, including those involved in perinuclear tethering, are implicated in heterochromatin propagation (32, 42). However, the mechanism remains to be fully elucidated. Here, we find that a critical threshold of H3K9me3 allows

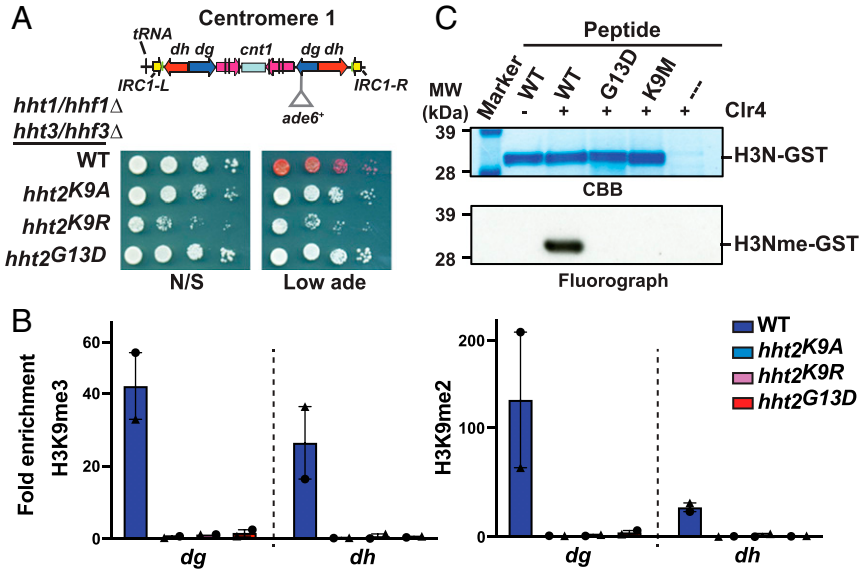

Fig. 4. $hht2^{G13D}$ impairs H3K9 methylation. (*A*) Expression analysis of *otr1R(Sph1)::ade6*$^{+}$ in the indicated strains. (*B*) ChIP-qPCR (mean ± SEM; $n = 2$) analysis showing the fold enrichment of H3K9me3 and H3K9me2 at *dg* and *dh* loci relative to *leu1* in the indicated *hht1/hhf1Δ hht3/hhf3Δ otr1R(Sph1)::ade6*$^{+}$ strains. (*C*) In vitro methylation assay of $H3^{G13D}$ and $H3^{K9M}$ substrates. Recombinant His_6-Clr4 was incubated with the indicated H3N-GST constructs and analyzed by SDS-PAGE followed by Coomassie Brilliant Blue (CBB) staining (*Top*) and fluorography (*Bottom*). Data are representative of two independent experiments. See also *SI Appendix*, Fig. S4.

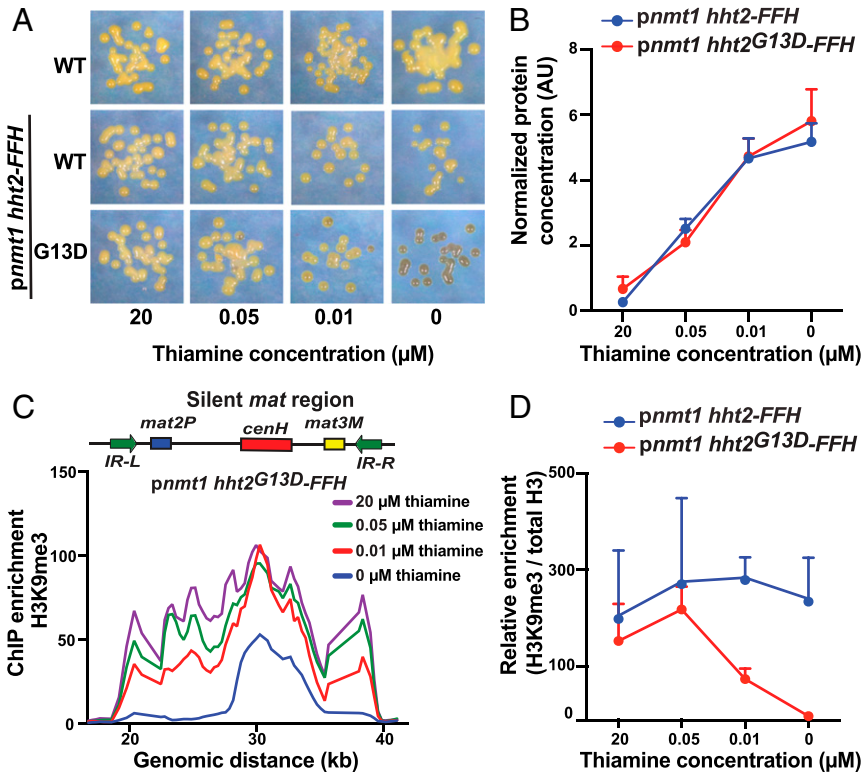

Fig. 5. $H3^{G13D}$ shows a dose-dependent effect on gene silencing and H3K9me3. (*A*) Detection of haploid meiosis in the indicated strain backgrounds. Cells were plated onto PMG media containing the indicated concentration of thiamine and stained with iodine vapor to detect haploid meiosis. Data are representative of three independent experiments. (*B*) Normalized protein concentrations (mean ± SEM; $n = 3$) determined by Western blot analysis of $H3\text{-}FLAG_2His_6$ (*hht2-FFH* and *hht2^{G13D}-FFH* strains) grown in PMG with the indicated concentration of thiamine. (*C*) ChIP-chip analysis of H3K9me3 enrichment at the silent *mat* locus in *REIIΔ mat2P::ura4$^+$ pnmt1 hht2G13D-FFH* strains grown in the absence or presence of the indicated concentration of thiamine, plotted using a sliding window average of three probes. (*D*) ChIP-qPCR (mean ± SEM; $n = 2$) analysis to determine relative fold enrichments of H3K9me3 at *mat2P* in the indicated *REIIΔ mat2P::ura4$^+$* strains. Relative fold enrichments were calculated as a ratio of fold enrichment of H3K9me3 at *mat2P* over total H3. See also *SI Appendix*, Fig. S5.

an effective local concentration of Clr4 to promote the read-write activity that supports spreading and maintenance of heterochromatin (Fig. 7).

We characterized a mutation that directly implicates H3K9me in the transmission of epigenetic memory. The dominant-negative *hht2^{G13D}* mutation affects heterochromatin propagation and results in a variegated phenotype. $H3^{G13D}$ is distinct from other histone mutants, including $H3^{K9M}$ that, in addition to blocking H3K9me, traps catalytic Clr4 to inhibit heterochromatin assembly (33). $H3^{G13D}$ cannot be methylated by Clr4 and disrupts the epigenetic loop mechanism involving Clr4 read-write activity. $H3^{G13D}$ directly blocks H3K9 methylation by Clr4, although it could impact ubiquitination of H3K14 that stimulates Clr4 activity (54). Regardless, $H3^{G13D}$ reduces the level of H3K9me3, which is required for the epigenetic-templated recruitment and stimulation of Clr4 enzymatic activity to promote heterochromatin propagation (22, 23). Consistently, $H3^{G13D}$ hinders the spread of ClrC and H3K9me from the nucleation site to surrounding regions in a dosage-dependent manner. Moreover, increasing the effective local concentration of Clr4 suppresses heterochromatin defects in *hht2^{G13D}* cells. A key finding, however, is that the $Clr4^{Chp1CD}$ chimeric protein, which can recognize H3K9me2 with high affinity, restores propagation of heterochromatin in *hht2^{G13D}* cells. In addition to underscoring the requirement for recognition of methylated H3K9 by Clr4 for heterochromatin propagation, these results reveal that a critical density of H3K9me3 supports epigenetic stability of repressive chromatin domains through the read-write mechanism.

The finding that a critical threshold of H3K9me3 is essential for faithful propagation of heterochromatin may shed light on how factors such as HP1, HDACs, and the anti-silencing factor Epe1 affect heterochromatin assembly. The oligomerization of HP1 (55) localized across heterochromatin domains might enhance the density of H3K9me3 nucleosomes and their associated Clr4 to promote the spreading and inheritance of heterochromatin. Similarly, deacetylation of histones by HDACs, such as Clr3, may promote nucleosome–nucleosome interactions and suppress histone turnover to enhance H3K9me3 density (29, 30, 56). Along these lines, Epe1 stimulates histone exchange (29) and therefore might lower H3K9me3 density to destabilize heterochromatin (43–45, 57). On other hand, perinuclear tethering of heterochromatin and phase separation might increase the local concentraton of modification-specific histone-binding proteins, including Clr4, to stabilize heterochromatin. In any case, maintaining a critical threshold of H3K9me3 is required for transgenerational inheritance of heterochromatin and stable gene silencing. Indeed, modified parental histones, which are deposited at their original location on daughter strands during replication (58, 59), are believed to recruit histone-modifying enzymes such as Clr4 to modify newly assembled nucleosomes (60).

Our findings may also illuminate mechanisms that maintain repressive chromatin domains in other systems. In particular, they may explain the recent observation in mouse embryonic stem cells that the linker histone H1 facilitates spreading of H3K9 methylation (61). In addition to the direct interaction between H1 and histone methyltransferases (61), stabilization of nucleosomes by

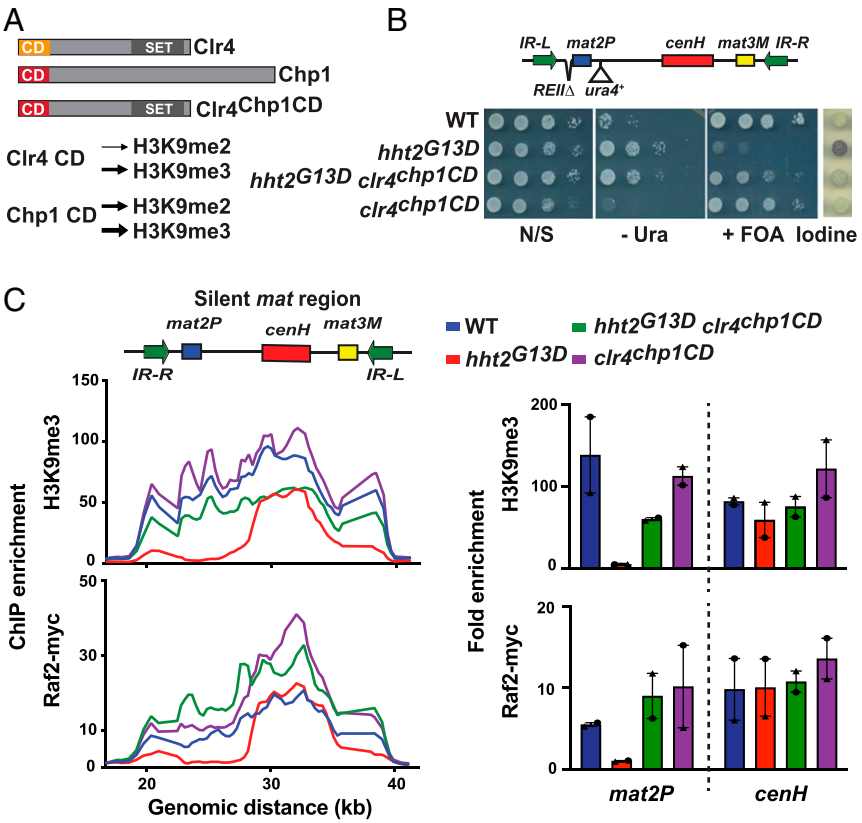

Fig. 6. Enhancing the affinity of Clr4 for H3K9me2 can suppress the heterochromatin spreading defect in cells expressing $H3^{G13D}$ mutant protein. (*A*) Schematic representation of chromodomain-containing Clr4 and Chp1 proteins as well as chimeric $Clr4^{Chp1CD}$. Their relative affinities for H3K9me2 and H3K9me3 are represented by arrow heads. (*B*) Expression analysis of *mat2P::ura4*$^+$ in the indicated strain backgrounds. Additionally, plates were stained with iodine vapor to detect haploid meiosis. (*C*) ChIP-chip analysis of H3K9me3 and Raf2-myc enrichment at the silent *mat* locus in the indicated *REIIΔ mat2P::ura4*$^+$ strains, plotted using a sliding window average of three probes. Raf2-myc data shown for WT and $hht2^{G13D}$ are also presented in Fig. 2*D* (*Left*). ChIP-qPCR (mean ± SEM; $n = 2$) analysis of H3K9me3 and Raf2-myc fold enrichment at *mat2P* and *cenH* in the indicated *REIIΔ mat2P::ura4*$^+$ strains (*Right*). See also *SI Appendix*, Figs. S6 and S7.

linker histones might preserve H3K9me3, which in turn facilitates anchoring of Suv39h1/2 via the chromodomain to promote spreading of heterochromatin. Similarly, dense chromatin was shown to facilitate PRC2-mediated H3K27 methylation (62). Although the mechanisms are likely to be more complex, histone K-to-M mutations frequently linked to cancer might compromise repressive chromatin assembly by affecting the local population of modified histones required to support the read-write activity of modifying enzymes (35, 36, 63, 64). Future studies will be needed to determine if a critical density of H3K9me3, which also facilitates DNA methylation (65), is a conserved requirement for the assembly and propagation of heterochromatin domains in other systems.

Materials and Methods

Strains, Media, and Plasmid Construction. *S. pombe* yeast strains used in this study are listed in *SI Appendix*, Table S1. Deletion and epitope-tagged strains were generated by standard PCR-based methodology and transformation or genetic crosses followed by tetrad dissection (*SI Appendix*). Standard techniques were used to culture *S. pombe*. All experiments were performed in yeast extract rich medium supplemented with adenine (YEA) at 32 °C unless indicated otherwise. For serial dilution assays, tenfold dilutions of a mid log-phase culture were plated on PMG (Pombe Minimal Glutamate medium), PMG − ura, or PMG + FOA and grown for 2 to 3 d at 30 to 32 °C unless stated otherwise. To assay for haploid meiosis, PMG or EMM (Edinburgh minimal medium) plates (incubated at 30 °C) were stained for 2 min with iodine vapor before imaging.

Ectopic Heterochromatin Silencing Assay. Strains containing *6xtetO-ade6+* inserted at the *ura4*$^+$ locus and *pnmt81-tetR*^{off}*-2xflag-clr4ΔCD* integrated at the *leu1*$^+$ locus were grown in EMM liquid media for 48 h to induce TetR-Clr4 expression and plated as tenfold serial dilutions on EMM low adenine (7.5 mg/L) medium with or without tetracyline (2.5 mg/L) to assess expression of *ade6*$^+$. For ChIP experiments, cells were were grown in EMM liquid media for 48 h to induce TetR-Clr4 expression and collected as 0 generation/– tetracyline samples or further grown in EMM + tetracycline (2.5 mg/L) liquid media for 4 or 10 generations, fixed, and processed for ChIP.

ChIP. ChIP experiments were performed as described previously (9) with some modifications (*SI Appendix*). Immunoprecipitated and input DNA were analyzed by performing qPCR or DNA microarray as described in *SI Appendix*.

Microscopy and Image Analysis. To quantify haploid meiosis, cells were collected from PMG plates grown at 30 °C for 2 to 3 d and imaged on a glass slide using a DeltaVision Elite microscope (GE Healthcare) with a 100× 1.4NA Plan Super Apochromat oil lens. Percent haploid meiosis was calculated by manually counting cells from images opened in Fiji.

Methyltransferase Assay. To examine the enzymatic activity of Clr4 on H3 peptide substrates (*SI Appendix*), histone methyltransferase assays were performed with equal microgram quantities of recombinant Clr4 and H3N-GST in methyltransferase buffer (50 mM Tris [pH 8.0], 10% glycerol, 1 mM DTT, 1 mM phenylmethylsulfonyl fluoride [PMSF]) supplemented with [^{3}H] labeled-SAM for 1 h at 30 °C. The samples were resolved by sodium dodecyl sulfate-polyacrylamide gel electrophoresis (SDS-PAGE) and stained with Coomassie to visualize the proteins. Gels were then treated with Amplify (GE Healthcare), dried, and subjected to fluorography to detect [^{3}H]-labeled substrates.

See *SI Appendix* for additional details and descriptions of genetic screening, Western blotting, protein purification, and mass spectrometry analyses.

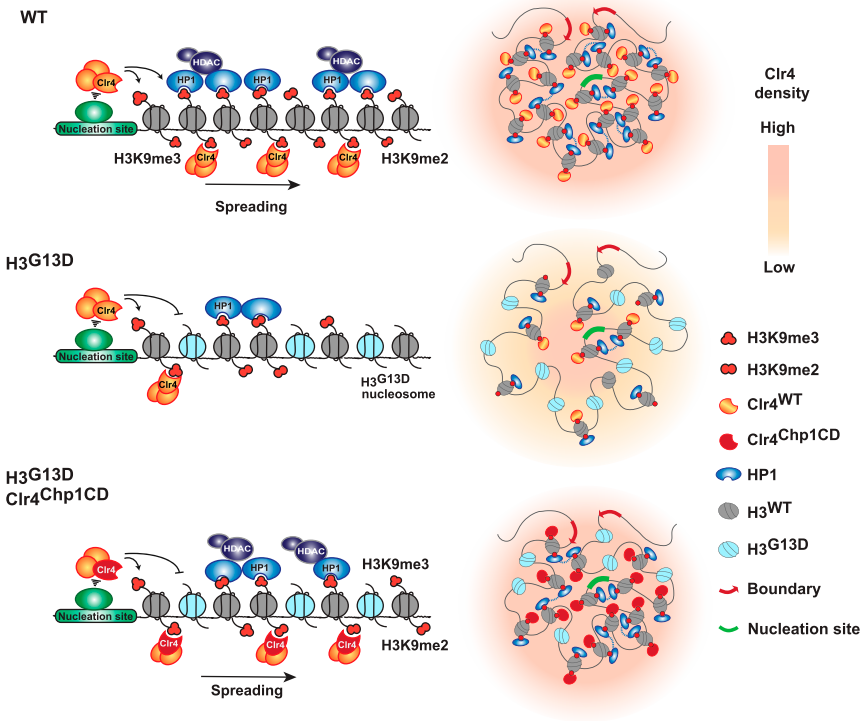

Fig. 7. Model showing how $H3^{G13D}$ affects the propagation of heterochromatin. At sites of nucleation, the RNAi machinery as well as RNAPII termination factors and DNA binding proteins recruit Clr4 that catalyzes mono-, di-, and tri-methylation of histone H3K9. HP1 bound to H3K9me bridges nucleosomes and recruits factors such as HDACs that suppress histone turnover to enhance the density of modified nucleosomes and their associated proteins, incuding Clr4. In WT cells, the high local concentration of Clr4 bound to H3K9me3 promotes the spreading and maintenance of heterochromatin via read-write activity (*Top*). The incorporation of $H3^{G13D}$ blocks H3K9me on the mutant histone H3, which reduces H3K9me3 density and compromises the read-write activity of Clr4, ultimately disrupting the propagation of heterochromatin (*Middle*). The reduced Clr4 retention on chromatin in $H3^{G13D}$ cells disproportionately affects the conversion of di- to tri-H3K9 methylation, which occurs relatively inefficiently and is more sensitive to Clr4 read-write activity. Expressing the $Clr4^{Chp1CD}$ chimeric protein, which can bind H3K9me2 with high affinity, reestablishes sufficient Clr4 density to restore heterochromatin spreading even in the presence of $H3^{G13D}$-containing nucleosomes (*Bottom*).

Data Availability. Microarray data are deposited in the Gene Expression Omnibus with accession number GSE162701.

ACKNOWLEDGMENTS. We thank T. Andresson and M. O'Neill for mass spectrometry analyses. We also thank J. Barrowman for editing the manuscript, H.D. Folco, M. Zofall, Y. Wei, H. Xiao, and members of the S.I.S.G. laboratory for technical assistance and helpful discussions and R. Allshire for strains. This study used the Helix Systems and Biowulf Linux cluster at the NIH. This work was supported by the Intramural Research Program of the NIH, National Cancer Institute.

1. T. Jenuwein, C. D. Allis, Translating the histone code. *Science* **293**, 1074–1080 (2001).
2. S. I. Grewal, S. Jia, Heterochromatin revisited. *Nat. Rev. Genet.* **8**, 35–46 (2007).
3. L. N. Rusche, A. L. Kirchmaier, J. Rine, The establishment, inheritance, and function of silenced chromatin in *Saccharomyces cerevisiae*. *Annu. Rev. Biochem.* **72**, 481–516 (2003).
4. S. R. Bhaumik, E. Smith, A. Shilatifard, Covalent modifications of histones during development and disease pathogenesis. *Nat. Struct. Mol. Biol.* **14**, 1008–1016 (2007).
5. Noma K, C. D. Allis, S. I. Grewal, Transitions in distinct histone H3 methylation patterns at the heterochromatin domain boundaries. *Science* **293**, 1150–1155 (2001).
6. J. Nakayama, J. C. Rice, B. D. Strahl, C. D. Allis, S. I. Grewal, Role of histone H3 lysine 9 methylation in epigenetic control of heterochromatin assembly. *Science* **292**, 110–113 (2001).
7. M. Lachner, D. O'Carroll, S. Rea, K. Mechtler, T. Jenuwein, Methylation of histone H3 lysine 9 creates a binding site for HP1 proteins. *Nature* **410**, 116–120 (2001).
8. A. J. Bannister *et al*., Selective recognition of methylated lysine 9 on histone H3 by the HP1 chromo domain. *Nature* **410**, 120–124 (2001).
9. H. P. Cam *et al*., Comprehensive analysis of heterochromatin- and RNAi-mediated epigenetic control of the fission yeast genome. *Nat. Genet.* **37**, 809–819 (2005).
10. P. S. Gallagher *et al*., Iron homeostasis regulates facultative heterochromatin assembly in adaptive genome control. *Nat. Struct. Mol. Biol.* **25**, 372–383 (2018).
11. J. Wang, B. D. Reddy, S. Jia, Rapid epigenetic adaptation to uncontrolled heterochromatin spreading. *eLife* **4**, e06179 (2015).
12. M. Zofall *et al*., RNA elimination machinery targeting meiotic mRNAs promotes facultative heterochromatin formation. *Science* **335**, 96–100 (2012).
13. I. M. Hall *et al*., Establishment and maintenance of a heterochromatin domain. *Science* **297**, 2232–2237 (2002).
14. M. J. Obersriebnig, E. M. Pallesen, K. Sneppen, A. Trusina, G. Thon, Nucleation and spreading of a heterochromatic domain in fission yeast. *Nat. Commun.* **7**, 11518 (2016).
15. T. A. Volpe *et al*., Regulation of heterochromatic silencing and histone H3 lysine-9 methylation by RNAi. *Science* **297**, 1833–1837 (2002).
16. V. R. Chalamcharla, H. D. Folco, J. Dhakshnamoorthy, S. I. Grewal, Conserved factor Dhp1/Rat1/Xrn2 triggers premature transcription termination and nucleates heterochromatin to promote gene silencing. *Proc. Natl. Acad. Sci. U.S.A.* **112**, 15548–15555 (2015).
17. S. Y. Lee *et al*., Dense transposon integration reveals essential cleavage and polyadenylation factors promote heterochromatin formation. *Cell Rep.* **30**, 2686–2698.e8 (2020).
18. J. F. Tucker *et al*., A novel epigenetic silencing pathway involving the highly conserved 5′-3′ exoribonuclease Dhp1/Rat1/Xrn2 in *Schizosaccharomyces pombe*. *PLoS Genet.* **12**, e1005873 (2016).
19. T. V. Vo *et al*., CPF recruitment to non-canonical transcription termination sites triggers heterochromatin assembly and gene silencing. *Cell Rep.* **28**, 267–281.e5 (2019).
20. P. J. Horn, J. N. Bastie, C. L. Peterson, A Rik1-associated, cullin-dependent E3 ubiquitin ligase is essential for heterochromatin formation. *Genes Dev.* **19**, 1705–1714 (2005).
21. T. Yamada, W. Fischle, T. Sugiyama, C. D. Allis, S. I. Grewal, The nucleation and maintenance of heterochromatin by a histone deacetylase in fission yeast. *Mol. Cell* **20**, 173–185 (2005).
22. K. Zhang, K. Mosch, W. Fischle, S. I. Grewal, Roles of the Clr4 methyltransferase complex in nucleation, spreading and maintenance of heterochromatin. *Nat. Struct. Mol. Biol.* **15**, 381–388 (2008).
23. B. Al-Sady, H. D. Madhani, G. J. Narlikar, Division of labor between the chromodomains of HP1 and Suv39 methylase enables coordination of heterochromatin spread. *Mol. Cell* **51**, 80–91 (2013).
24. M. Sadaie, T. Iida, T. Urano, J. Nakayama, A chromodomain protein, Chp1, is required for the establishment of heterochromatin in fission yeast. *EMBO J.* **23**, 3825–3835 (2004).

25. T. Sugiyama *et al*., SHREC, an effector complex for heterochromatic transcriptional silencing. *Cell* **128**, 491–504 (2007).
26. G. Job *et al*., SHREC silences heterochromatin via distinct remodeling and deacetylation modules. *Mol. Cell* **62**, 207–221 (2016).
27. S. I. Grewal, A. J. Klar, Chromosomal inheritance of epigenetic states in fission yeast during mitosis and meiosis. *Cell* **86**, 95–101 (1996).
28. J. Nakayama, A. J. Klar, S. I. Grewal, A chromodomain protein, Swi6, performs imprinting functions in fission yeast during mitosis and meiosis. *Cell* **101**, 307–317 (2000).
29. O. Aygün, S. Mehta, S. I. Grewal, HDAC-mediated suppression of histone turnover promotes epigenetic stability of heterochromatin. *Nat. Struct. Mol. Biol.* **20**, 547–554 (2013).
30. N. Taneja *et al*., SNF2 family protein Fft3 suppresses nucleosome turnover to promote epigenetic inheritance and proper replication. *Mol. Cell* **66**, 50–62.e6 (2017).
31. R. R. Barrales, M. Forn, P. R. Georgescu, Z. Sarkadi, S. Braun, Control of heterochromatin localization and silencing by the nuclear membrane protein Lem2. *Genes Dev.* **30**, 133–148 (2016).
32. S. Holla *et al*., Positioning heterochromatin at the nuclear periphery suppresses histone turnover to promote epigenetic inheritance. *Cell* **180**, 150–164.e15 (2020).
33. C. M. Shan *et al*., A histone H3K9M mutation traps histone methyltransferase Clr4 to prevent heterochromatin spreading. *eLife* **5**, e17903 (2016).
34. S. Behjati *et al*., Distinct H3F3A and H3F3B driver mutations define chondroblastoma and giant cell tumor of bone. *Nat. Genet.* **45**, 1479–1482 (2013).
35. H. M. Herz *et al*., Histone H3 lysine-to-methionine mutants as a paradigm to study chromatin signaling. *Science* **345**, 1065–1070 (2014).
36. P. W. Lewis *et al*., Inhibition of PRC2 activity by a gain-of-function H3 mutation found in pediatric glioblastoma. *Science* **340**, 857–861 (2013).
37. B. A. Nacev *et al*., The expanding landscape of 'oncohistone' mutations in human cancers. *Nature* **567**, 473–478 (2019).
38. J. Schwartzentruber *et al*., Driver mutations in histone H3.3 and chromatin remodelling genes in paediatric glioblastoma. *Nature* **482**, 226–231 (2012).
39. G. Wu *et al*.; St. Jude Children's Research Hospital–Washington University Pediatric Cancer Genome Project, Somatic histone H3 alterations in pediatric diffuse intrinsic pontine gliomas and non-brainstem glioblastomas. *Nat. Genet.* **44**, 251–253 (2012).
40. S. Matsumoto, M. Yanagida, Histone gene organization of fission yeast: A common upstream sequence. *EMBO J.* **4**, 3531–3538 (1985).
41. G. Thon, A. Cohen, A. J. Klar, Three additional linkage groups that repress transcription and meiotic recombination in the mating-type region of *Schizosaccharomyces pombe*. *Genetics* **138**, 29–38 (1994).
42. H. D. Folco, A. McCue, V. Balachandran, S. I. S. Grewal, Cohesin impedes heterochromatin assembly in fission yeast cells lacking Pds5. *Genetics* **213**, 127–141 (2019).
43. N. Ayoub *et al*., A novel jmjC domain protein modulates heterochromatization in fission yeast. *Mol. Cell. Biol.* **23**, 4356–4370 (2003).
44. P. N. Audergon *et al*., Epigenetics. Restricted epigenetic inheritance of H3K9 methylation. *Science* **348**, 132–135 (2015).
45. K. Ragunathan, G. Jih, D. Moazed, Epigenetics. Epigenetic inheritance uncoupled from sequence-specific recruitment. *Science* **348**, 1258699 (2015).
46. G. Shipkovenska, A. Durango, M. Kalocsay, S. P. Gygi, D. Moazed, A conserved RNA degradation complex required for spreading and epigenetic inheritance of heterochromatin. *eLife* **9**, e54341 (2020).
47. J. Kanoh, M. Sadaie, T. Urano, F. Ishikawa, Telomere binding protein Taz1 establishes Swi6 heterochromatin independently of RNAi at telomeres. *Curr. Biol.* **15**, 1808–1819 (2005).
48. T. S. van Emden *et al*., Shelterin and subtelomeric DNA sequences control nucleosome maintenance and genome stability. *EMBO Rep.* **20**, e47181 (2019).
49. J. Wang *et al*., The proper connection between shelterin components is required for telomeric heterochromatin assembly. *Genes Dev.* **30**, 827–839 (2016).
50. M. Zofall, D. R. Smith, T. Mizuguchi, J. Dhakshnamoorthy, S. I. S. Grewal, Taz1-Shelterin promotes facultative heterochromatin assembly at chromosome-internal sites containing late replication origins. *Mol. Cell* **62**, 862–874 (2016).
51. X. Tadeo *et al*., Elimination of shelterin components bypasses RNAi for pericentric heterochromatin assembly. *Genes Dev.* **27**, 2489–2499 (2013).
52. B. G. Mellone *et al*., Centromere silencing and function in fission yeast is governed by the amino terminus of histone H3. *Curr. Biol.* **13**, 1748–1757 (2003).
53. T. Schalch *et al*., High-affinity binding of Chp1 chromodomain to K9 methylated histone H3 is required to establish centromeric heterochromatin. *Mol. Cell* **34**, 36–46 (2009).
54. E. Oya *et al*., H3K14 ubiquitylation promotes H3K9 methylation for heterochromatin assembly. *EMBO Rep.* **20**, e48111 (2019).
55. D. Canzio *et al*., Chromodomain-mediated oligomerization of HP1 suggests a nucleosome-bridging mechanism for heterochromatin assembly. *Mol. Cell* **41**, 67–81 (2011).
56. R. A. Greenstein *et al*., Noncoding RNA-nucleated heterochromatin spreading is intrinsically labile and requires accessory elements for epigenetic stability. *eLife* **7**, e32948 (2018).
57. M. Zofall, S. I. Grewal, Swi6/HP1 recruits a JmjC domain protein to facilitate transcription of heterochromatic repeats. *Mol. Cell* **22**, 681–692 (2006).
58. T. M. Escobar *et al*., Active and repressed chromatin domains exhibit distinct nucleosome segregation during DNA replication. *Cell* **179**, 953–963.e11 (2019).
59. D. S. Saxton, J. Rine, Nucleosome positioning regulates the establishment, stability, and inheritance of heterochromatin in *Saccharomyces cerevisiae*. *Proc. Natl. Acad. Sci. U.S.A.* **117**, 27493–27501 (2020).
60. A. Serra-Cardona, Z. Zhang, Replication-coupled nucleosome assembly in the passage of epigenetic information and cell identity. *Trends Biochem. Sci.* **43**, 136–148 (2018).
61. S. E. Healton *et al*., H1 linker histones silence repetitive elements by promoting both histone H3K9 methylation and chromatin compaction. *Proc. Natl. Acad. Sci. U.S.A.* **117**, 14251–14258 (2020).
62. W. Yuan *et al*., Dense chromatin activates Polycomb repressive complex 2 to regulate H3 lysine 27 methylation. *Science* **337**, 971–975 (2012).
63. A. S. Harutyunyan *et al*., H3K27M induces defective chromatin spread of PRC2-mediated repressive H3K27me2/me3 and is essential for glioma tumorigenesis. *Nat. Commun.* **10**, 1262 (2019).
64. S. U. Jain *et al*., H3 K27M and EZHIP impede H3K27-methylation spreading by inhibiting allosterically stimulated PRC2. *Mol. Cell* **80**, 726–735.e7 (2020).
65. H. Tamaru *et al*., Trimethylated lysine 9 of histone H3 is a mark for DNA methylation in *Neurospora crassa*. *Nat. Genet.* **34**, 75–79 (2003).